Applied Surface Science 422 (2017) 661–665

Contents lists available at ScienceDirect

Applied Surface Science

journal homepage: www.elsevier.com/locate/apsusc

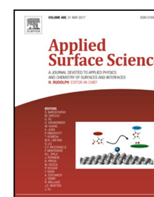

Full Length Article

ALD synthesis of platinum nanoparticles on single-crystal $SrTiO_3$ pretreated with wet chemical etching

Chuandao Wang [a,*], Pratik Koirala [a], Peter Stair [b], Laurence Marks [a]

[a] *Department of Materials Science and Engineering, Northwestern University, 2220 North Campus Drive, Evanston, IL 60208-3108, USA*
[b] *Department of Chemistry, Northwestern University,2145 Sheridan Road, Evanston, IL 60208-3113, USA*

ARTICLE INFO

Article history:
Received 1 March 2017
Received in revised form 20 May 2017
Accepted 22 May 2017
Available online 1 June 2017

Keywords:
Platinum
Atomic layer deposition
Etch
Surface condition

ABSTRACT

Formic acid-hydrogen peroxide and buffered hydrogen fluoride-hydrogen peroxide solutions were used to etch single-crystal strontium titanate to remove carbon contamination and increase hydroxyl group density to improve atomic layer deposition onto these materials. X-ray photoelectron spectroscopy indicated that both are effective for carbon contamination removal. However, for increasing hydroxyl group density on the strontium titanate surface, the buffered hydrogen fluoride-hydrogen peroxide is more effective. Transmission electron microscopy and x-ray photoemission show enhanced platinum deposition on the etched strontium titanate surface. These results provide the basis for optimizing atomic layer deposition for other technologically relevant materials.

© 2017 Elsevier B.V. All rights reserved.

1. Introduction

Atomic layer deposition (ALD) is widely employed for the growth of atomically smooth, conformal thin films [1,2] and metal nanoparticles [3,4] on nanoparticle support for applications in catalysis [4–6] and sensing [7–12]. ALD on single crystalline (SC) substrates such as $SrTiO_3$ (STO) has applications in dynamic random access memory [13,14], field effect transistors [15,16] and ferroelectric devices [17,18]. SC substrates are also ideal for quantification of catalytic performance and precursor-substrate interactions (e.g. photocatalytic water splitting [19–21]) as they provide a relatively more controlled surface than a nanoparticle support.

However, deposition of ALD material on bulk SC substrates is challenging due to the limited surface to volume ratio. Precursor sticking coefficient on large surfaces is also deteriorated by surface contaminants such as carbon [22]. Ratio of C to Sr X-ray photoelectron spectroscopy (XPS) [23] peak intensity has indicated a uniform coverage of C on STO (001) surface owing to atmospheric exposure. Standard cleaning procedures such as ion sputtering and annealing [24,25] induce radiation damage [26] and significantly reduce surface hydroxyl concentration which is a prerequisite for many ALD recipes. It is therefore imperative to design alternative approaches that provide clean hydroxyl enriched surfaces.

Wet chemical etching is commonly used for the preparation of atomically flat crystalline substrates. For instance, both BHF and Arkansas [28] etching solutions yield an atomically smooth TiO_2 terminated surface on (001) STO [29,30]. In this study, we propose the use of formic acid-hydrogen peroxide (FA-HP) and buffered hydrogen fluoride-hydrogen peroxide (BHF-HP) etching solutions for the surface treatment of $SrTiO_3$ prior to ALD. TEM and XPS characterization indicate BHF-HP solution to be more effective in reducing carbon contamination and increasing surface hydroxide density, thereby enhancing ALD growth.

2. Methods

SC STO (001) substrates with one side Epi [31] polished were purchased from MTI Corp. (Richmond, California), and cut into 3 mm discs, mechanically polished and ion beam milled to electron transparency. Initial ion milling was done with high energy Ar ions (~6 keV) and gradually reduced to 2.5–3 keV for final polishing. Transmission electron microscopy (TEM) analysis was performed using a JEOL-JEM 2100F operated at 200 kV.

One as-received Epi polished and one mechanically polished substrate was used to study the surface compositional changes as a function of treatment. Two other samples were subjected to wet chemical etching: one with buffered hydrogen fluoride-hydrogen peroxide (BHF-HP, 70% commercial buffered HF, 30% H_2O_2 by volume) and the other with formic acid-hydrogen peroxide (FA-HP, 60% formic acid, 30% H_2O_2, 10% Deionized water by volume).

* Corresponding author.
E-mail address: ericenkin@gmail.com (C. Wang).

http://dx.doi.org/10.1016/j.apsusc.2017.05.187
0169-4332/© 2017 Elsevier B.V. All rights reserved.

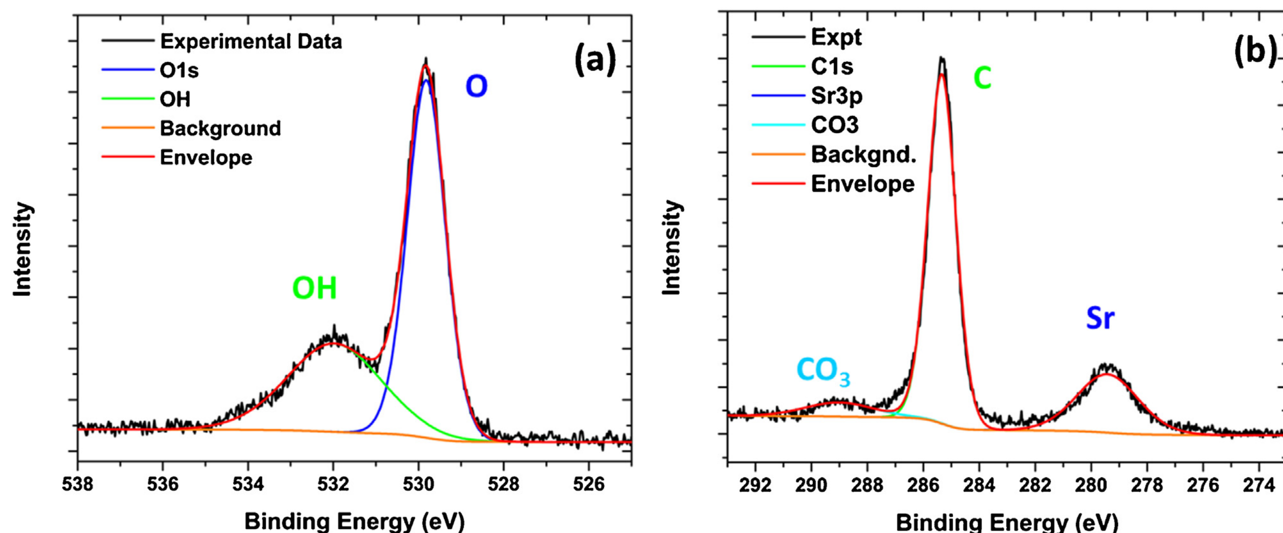

Fig. 1. (a) O 1 s core level XPS peaks of SC-STO with Gaussian profiles denoted as O1 s (~530 eV) and OH (532.2 eV), respectively; (b) C 1 s (285 eV) and Sr 3p1/2 (279.5 eV), CO3 peak is contributed by SrCO3 carbonates. XPS peaks of SC-STO with Gaussian profiles denoted. (These results are from a sample treated in BHF-HP for 1 min.).

Fig. 2. Evolution of surface (a) hydroxyl and (b) carbon concentration with BHF-HP, FA-HP etching at room temperature, (c) hydroxyl and (d) carbon concentration with BHF-HP etching at elevated temperature on SC-STO (001) surface.

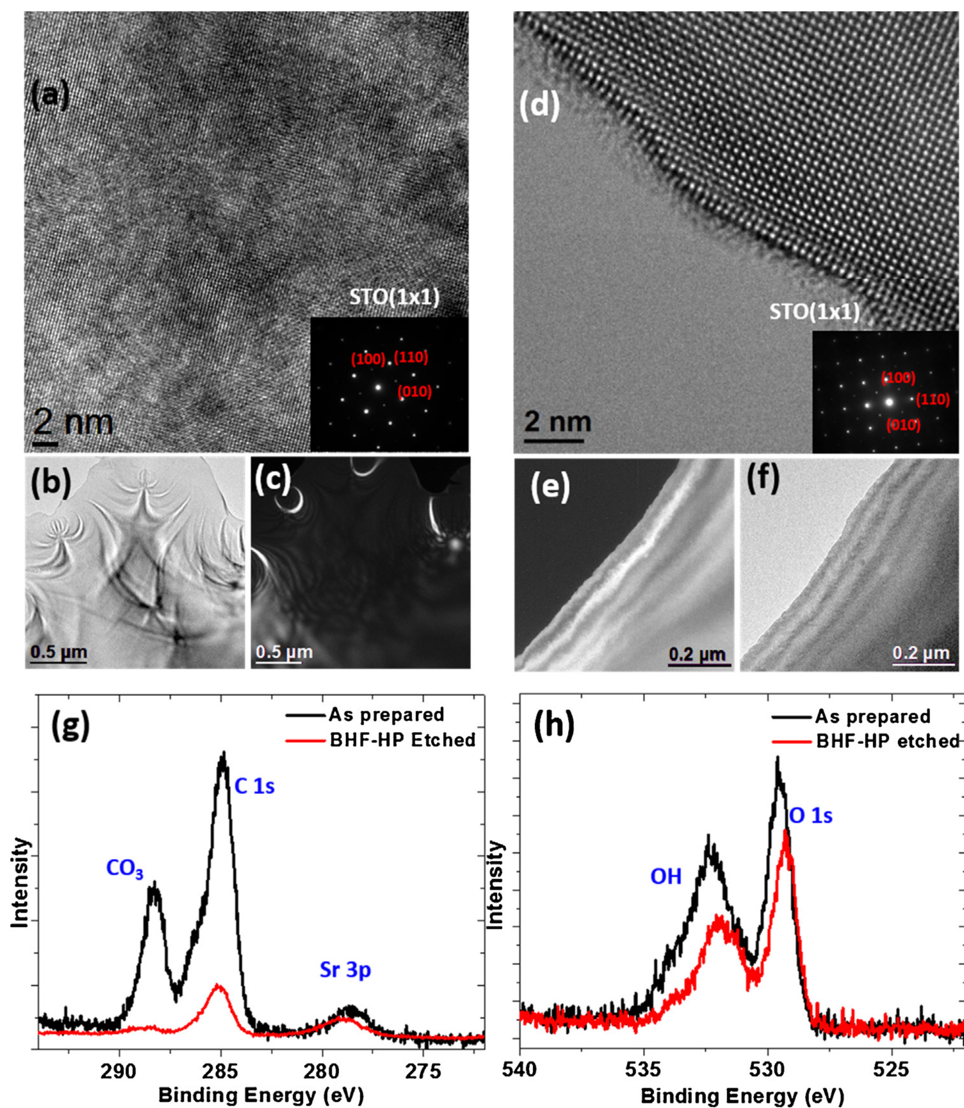

Fig. 3. (a) HRTEM with inserted diffraction pattern, (b) bright field and (c) dark field image of as-prepared SC-STO TEM sample and (d) HRTEM with inserted diffraction pattern, (e) dark field and (f) bright field image of BHF-HP etched SC-STO TEM sample. XPS spectra of (g) C1 s (h) O1 s peaks of as prepared and BHF etched TEM samples.

Quantification of carbon contamination and surface hydroxyl density was done using XPS (Thermo-Scientific EXCALAB 250 Xi), equipped with a monochromated, micro-focused Al K-Alpha source of spot size 300 μm and energy resolution of 0.5 eV. An Ar flood gun was used for charge compensation. The binding energy shift due to residual charging was corrected with respect to the Ti 2p3/2 peak referenced at 458.8 eV. XPS peaks were deconvoluted following a background subtraction using the Shirley algorithm with constrains on the peak positions.

Pt ALD was accomplished via alternating exposures to methylcyclopentadienyl trimethylplatinum ($MeCpPtMe_3$, Sigma-Aldrich 99%) and water. All reactions were carried out in a viscous flow reaction chamber at 250 °C by passing 120 sccm of ultrahigh purity (99.995% pure) N_2 at a steady state pressure of 1 Torr. Each ALD cycle was comprised of a 300 s exposure to $MeCpPtMe_3$ (heated to 50 °C) under 5 sccm flow of N_2, a 600 s N_2 purge, a 120 s exposure to H_2O(Room Temperature), and a 600 s N_2 purge.

3. Results

The concentrations of surface hydroxyl groups and carbon contamination were measured via the ratio of intensities of the OH shoulder to the O 1 s peak (Fig. 1a) and the C 1 s peak to the Sr 3p1/2 peak, respectively (Fig. 1b). The results from annealing and different chemical treatments are given in Fig. 2. Annealing of an as-receive Epi polished sample at 700 °C in air for 240 min removed 17 atomic% carbon contamination and 16 atomic% surface hydroxyl. (Hereafter we will use% for atomic%.) Mechanical polishing increased the surface carbon contamination (+%12) and hydroxyl density (+51%) simultaneously (Fig. 2), similar annealing of these samples reduced 30% carbon and 23% surface hydroxyl.

Two wet chemical etching experiments were also performed at room temperature on two different samples: a 20 min (min) etch in BHF-HP removed 32% carbon contamination and 64% surface hydroxyls, and a 20 min FA-HP etch removed 40% carbon and 59% hydroxyls. In either case, simultaneous removal of hydroxyl and carbon groups and greater reduction of carbon than hydroxyl group suggests that the initially removed hydroxyl groups are absorbed on carbon species. A subsequent 20 min etch in either of these two solutions resulted in further removal of carbon while the density of hydroxyl groups began to increase indicating a direct adsorption of hydroxyl groups on the clean STO surface. Longer etching time (> 40 min) with BHF-HP further removed carbon and increased the

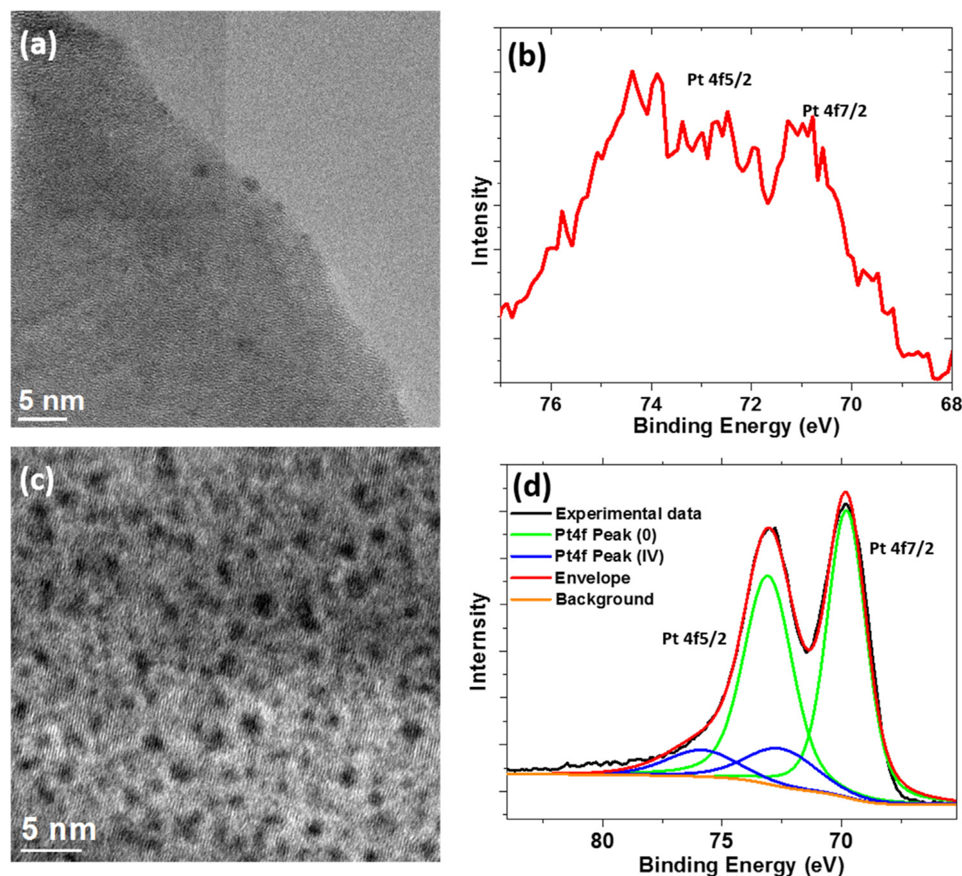

Fig. 4. HRTEM of 5 cycles ALD Pt nanoparticles on (a) as-prepared TEM sample (c) BHF-HP etched sample. XPS Pt 4f peaks of Pt deposited on (b) as prepared sample and (d) BHF-HP etched sample.

surface hydroxyl coverage while etching in FA-HP saturated after 40 min.

BHF-HP etching of SC-STO is a combination of two processes: BHF etching of SrO layers [30] and HP oxidative removal of carbon [32]. As demonstrated by Kawasaki et al. [30], SrO, a basic oxide, can be easily removed by a pH controlled BHF etch leaving behind a TiO_2 rich surface. HP on the other hand is a source of highly reactive hydroxyl radicals via photolysis process, HOOH + h$\upsilon \rightarrow$ 2*OH [32]. The hydroxyl radical is able to degrade and oxidize carbon contamination which contributes to the carbon removal [33]. With the increase of TiO_2 coverage after SrO removal, photon mediated holes on the TiO_2 surface can combine with the hydroxyl ion to produce extra radicals (OH^- + h$\upsilon \rightarrow$ *OH) besides the photolysis process of HP which can further the carbon removal process [34,35]. However exhaustion of hydrogen peroxide occurred around 40 min of etching slows down the removal of carbon as shown in Fig. 2. The surface hydroxyl density increases during the latter 20 min of BHF-HP etching is through photon induced hydrophilicity of newly formed TiO_2 layer [36] post SrO layer removal by BHF. Carbon removal via wet chemical etching is a kinetic process which depends on etching temperature [37]. The results in Fig. 2 from etching in BHF-HP show higher removal rates at 45 °C than at room temperature. The removal of carbon can be described by an Arrhenius relation,

$$K = t \exp\left(-\frac{E_a}{kT}\right)$$

where t is the pre-exponential constant, K is the etch rate, E_a is the activation energy, k is the Boltzmann constant and T is the etching temperature in degrees Kelvin. Based on Fig. 2, the carbon removal activation energy was calculated to be approximately 0.38 eV (36.58 kJ/mol).

Plan-view TEM and XPS were used to study the morphology and composition of an as-prepared and a BHF-HP etched (40 min at 45 °C) STO samples before ALD deposition (Fig. 3). The high resolution transmission electron microscopy (HRTEM) image in Fig. 3a shows lattice damage in the as prepared sample after ion milling, observable by local changes in the contrast. Similar effects from the damage are apparent in the bright field and dark field images in Fig. 3b and c in the extinction contours which indicate strain contrast from point defects and bulk incorporation of argon. The HRTEM image in Fig. 3d as well as the bright and dark field images of Fig. 3e and f shows reduction in lattice damage and the strain contrast following a BHF-HP etch. XPS spectra of an as-prepared and a BHF-HP etched STO samples before ALD (Fig. 3g, h) indicates higher surface hydroxyl and carbon on the as-prepared STO than the BHF-HP etched sample. In spite of the higher hydroxyl concentration, ALD deposition of Pt on as-prepared substrates is still more difficult as the adsorption of Pt precursor is sterically hindered by carbon contamination [38].

Fig. 4a and c shows HRTEM images of Pt deposited on the as-prepared and the BHF-HP etched STO samples after 5 ALD cycles. In order to distinguish Pt nanoparticles from the substrate in HRTEM, the sample was tilted off the low index zone axis. The images clearly show Pt as discrete nanoparticles with an average size of approximately ~2.0 nm on either sample which is consistent with the reported size of Pt nanoparticle deposited on strontium titanate nanocuboids in other work [39]. In contrast to the BHF-HP etched substrate, very few Pt nanoparticles were found on the as-prepared substrate. The XPS Pt 4f spectra in Fig. 4d show that the Pt deposited on the BHF-HP etched sample is mostly Pt(0) (~88%) with a small fraction of Pt(IV) (~12%). Sparse Pt loading on the as-prepared sam-

Table 1
Summary of XPS analysis of 5 cycles Pt deposited on two type of SC-STO sample.

	Pt/BHF-HP etch sample	Pt/As-prepared sample
Pt 4f/Ti 2p	0.237	0.015
C 1s/Ti 2p	1.322	3.438
Ti 2p/Sr 3d	1.066	0.900

ple led to a low signal to noise ratio for the Pt 4f peak (Fig. 4b) making reliable quantification difficult. Quantification of XPS data (Table 1) was done by comparing signal intensities, taking into account the corresponding sensitivity factors. These results show that BHF-HP etching improved the average Pt deposition per cycle by a factor of ~15. Carbon contamination on the BHF-HP etched sample was 60% less than on as-prepared samples and BHF etched sample yield a surface more Ti rich than FA.

4. Conclusion

Using TEM and XPS, we have demonstrated that more Pt is deposited via ALD on a BHF-HP etched surface than an untreated surface. BHF-HP etching of STO surfaces efficiently removes carbon contamination and increases surface hydroxyl group. A clean hydroxyl rich surface exhibits enhanced Pt precursor adsorption, thus yielding higher particle density. The chemical treatment detailed in this paper can potentially be expanded for surface preparation of other substrates such as silicon, barium titanate, titanium dioxide to optimize ALD deposition. However, the ideal etching solution may vary depending on the surface chemical properties of the target material.

Acknowledgements

CW acknowledges funding from the Northwestern University Institute for Catalysis in Energy Processes (ICEP) on grant number DOE DE-FG02-03-ER15457; PK acknowledges funding from the NSF on grant number DMR-1206320.

References

[1] A.R. Akbashev, G.N. Chen, J.E. Spanier, Nano Lett. 14 (1) (2014) 44–49.
[2] M. Aaltonen, T. Sajavaara, J. Keinonen, M. Leskela, Chem Mater. 15 (9) (2003) 1924–1928.
[3] S.T. Christensen, J.W. Elam, F.A. Rabuffetti, Q. Ma, S.J. Weigand, B. Lee, S. Seifert, P.C. Stair, K.R. Poeppelmeier, M.C. Hersam, M.J. Bedzyk, Small 5 (6) (2009) 750–757.
[4] J.A. Enterkin, K.R. Poeppelmeier, L.D. Marks, Nano Lett. 11 (3) (2011) 993–997.
[5] S.T. Christensen, H. Feng, J.L. Libera, N. Guo, J.T. Miller, P.C. Stair, J.W. Elam, Nano Lett. 10 (8) (2010) 3047–3051.
[6] J. Keranen, A. Auroux, S. Ek, L. Niinisto, Appl. Catal. A: Gen. 228 (1–2) (2002) 213–225.
[7] S. Cho, D.H. Kim, B.S. Lee, J. Jung, W.R. Yu, S.H. Hong, S. Lee, Sens. Actuators, B 162 (1) (2012) 300–306.
[8] I.J.M. Erkens, M.A. Blauw, M.A. Verheijen, F. Roozeboom, W.M.M. Kessels, Ecs Transactions 58 (10) (2013) 203–214.
[9] J.W. Elam, N.P. Dasgupta, F.B. Prinz, Materials Research Society Bulletin 36 (11) (2011) 899–906.
[10] M. Knez, K. Niesch, L. Niinisto, Adv. Mater. 19 (21) (2007) 3425–3438.
[11] S.M. George, Chem. Rev. 110 (1) (2010) 111–131.
[12] V. Miikkulainen, O. Nilsen, M. Laitinen, T. Sajavaara, H. Fjellvag, RSC Adv. 3 (20) (2013) 7537–7542.
[13] D. Roy, S.B. Krupanidhi, Appl. Phys. Lett. 62 (10) (1993) 1056–1058.
[14] S.B. Krupanidhi, G.M. Rao, Thin Solid Films 249 (1) (1994) 100–108.
[15] H. Yan, T. Jo, H. Okuzaki, Jpn. J. Appl. Phys. 49 (3) (2010) 030203.
[16] K. Uchida, A. Yoshikawa, K. Koumoto, T. Kato, Y. Ikuhara, H. Ohta, J. Appl. Phys. 107 (9) (2010) 096103.
[17] X. Marti, F. Sanchez, D. Hrabovsky, J. Fontcuberta, V. Laukhin, V. Skumryev, M.V. Garcia-Cuenca, C. Ferrater, M. Varela, U. Luders, J.F. Bobo, S. Estrade, J. Arbiol, F. Peiro, J. Cryst. Growth 299 (2) (2007) 288–294.
[18] S. Schmidt, Y.W. Ok, D.O. Klenov, J.W. Lu, S.P. Keane, S. Stemmer, J. Mater. Res. 20 (9) (2005) 2261–2265.
[19] R.G. Carr, G.A. Somorjai, Nature 290 (5807) (1981) 576–577.
[20] F.T. Wagner, S. Ferrer, G.A. Somorjai, Surf. Sci. 101 (1-3) (1980) 462–474.
[21] F.T. Wagner, G.A. Somorjai, J. Am. Chem. Soc. 102 (17) (1980) 5494–5502.
[22] E. Loginova, N.C. Bartelt, P.J. Feibelman, K.F. McCarty, New J Phys 11 (2009) 063046.
[23] V. Fouquet-Parry, F. Paumier, M.J. Guittet, M. Gautier-Soyer, J. Phys.: Conf. Ser. 94 (1) (2008) 012010.
[24] Z. Novotny, N. Mulakaluri, Z. Edes, M. Schmid, R. Pentcheva, U. Diebold, G.S. Parkinson, Phys. Rev. B 88 (3) (2013) 195410.
[25] P. Jacobson, S.C. Li, C. Wang, U. Diebold, J. Vac. Sci. Technol. B 26 (6) (2008) 2236–2240.
[26] O. Dulub, M. Batzill, S. Solovev, E. Loginova, A. Alchagirov, T.E. Madey, U. Diebold, Science 317 (5841) (2007) 1052–1056.
[28] M. Kareev, S. Prosandeev, J. Liu, C. Gan, A. Kareev, J.W. Freeland, M. Xiao, J. Chakhalian, Appl. Phys. Lett. 93 (6) (2008) 061909.
[29] R.H. Chae, R.A. Rao, Q. Gan, C.B. Eom, J. Electroceram. 4 (2–3) (2000) 345–349.
[30] M. Kawasaki, K. Takahashi, T. Maeda, R. Tsuchiya, M. Shinohara, O. Ishiyama, T. Yonezawa, M. Yoshimoto, H. Koinuma, Science 266 (5190) (1994) 1540–1542.
[31] G.P. Sahoo, H. Bar, D.K. Bhui, P. Sarkar, S. Samanta, S. Pyne, S. Ash, A. Misra, Coll. Surf. A 375 (1–3) (2011) 30–34.
[32] T. Hullar, C. Anastasio, Atmos. Chem. Phys. 11 (14) (2011) 7209–7222.
[33] C.A. Cantrell, R.E. Shetter, A.H. Mcdaniel, J.G. Calvert, J.A. Davidson, D.C. Lowe, S.C. Tyler, R.J. Cicerone, J.P. Greenberg, J. Geophys. Res. 95 (D13) (1990) 22455–22462.
[34] J.J. Wang, X.N. Liu, R.H. Li, P.S. Qiao, L.P. Xiao, J. Fan, Catal. Commun. 19 (2012) 96–99.
[35] M.E. Simonsen, Z.S. Li, E.G. Sogaard, Appl. Surf. Sci. 255 (18) (2009) 8054–8062.
[36] K. Takahashi, H. Yui, J. Phys. Chem. C 113 (47) (2009) 20322–20327.
[37] J.M. Ortion, Y. Cordier, J.C. Garcia, J. Cryst. Growth 164 (1-4) (1996) 97–103.
[38] Y.J. Chen, H.D. Kaesz, Appl. Phys. Lett. 53 (17) (1988) 1591–1592.
[39] C.D. Wang, L.H. Hu, Nanotechnology 28 (18) (2017) 185704.